Protein Science (1995), *4*:2366–2374. Cambridge University Press. Printed in the USA.
Copyright © 1995 The Protein Society

Active site model for γ-aminobutyrate aminotransferase explains substrate specificity and inhibitor reactivities

MICHAEL D. TONEY,[1,2] STEFANO PASCARELLA,[2] AND DANIELA DE BIASE[2]

[1] Department of Biochemistry, Albert Einstein College of Medicine, Bronx, New York 10461-1602
[2] Dipartimento di Scienze Biochimiche "A. Rossi Fanelli" and CNR, Centro di Biologia Molecolare, Università di Roma "La Sapienza," Piazzale Aldo Moro, 5-00185 Roma, Italy

(RECEIVED June 21, 1995; ACCEPTED August 16, 1995)

Abstract

A homology model for the pig isozyme of the pyridoxal phosphate-dependent enzyme γ-aminobutyrate (GABA) aminotransferase has been built based mainly on the structure of dialkylglycine decarboxylase and on a multiple sequence alignment of 28 evolutionarily related enzymes. The proposed active site structure is presented and analyzed. Hypothetical structures for external aldimine intermediates explain several characteristics of the enzyme. In the GABA external aldimine model, the pro-*S* proton at C4 of GABA, which abstracted in the 1,3-azaallylic rearrangement interconverting the aldimine and ketimine intermediates, is oriented perpendicular to the plane of the pyridoxal phosphate ring. Lys 329 is in close proximity and is probably the general base catalyst for the proton transfer reaction. The carboxylate group of GABA interacts with Arg 192 and Lys 203, which determine the specificity of the enzyme for monocarboxylic ω-amino acids such as GABA. In the proposed structure for the L-glutamate external aldimine, the α-carboxylate interacts with Arg 445. Glu 265 is proposed to interact with this same arginine in the GABA external aldimine, enabling the enzyme to act on ω-amino acids in one half-reaction and on α-amino acids in the other. The reactivities of inhibitors are well explained by the proposed active site structure. The *R* and *S* isomers of β-substituted phenyl and *p*-chlorophenyl GABA would bind in very different modes due to differential steric interactions, with the reactive *S* isomer leaving the orientation of the GABA moiety relatively unperturbed compared to that of the natural substrate. In our model, only the reactive *S* isomer of the mechanism-based inhibitor vinyl-GABA, an effective anti-epileptic drug known clinically as Vigabatrin, would orient the scissile C4-H bond perpendicular to the coenzyme ring plane and present the proton to Lys 329, the proposed general base catalyst of the reaction. The *R* isomer would direct the vinyl group toward Lys 329 and the C4-H bond toward Arg 445. The active site model presented provides a basis for site-directed mutagenesis and drug design experiments.

Keywords: γ-aminobutyrate aminotransferase; GABA; homology modeling; pyridoxal phosphate; Vigabatrin

γ-Aminobutyrate aminotransferase is a pyridoxal phosphate-dependent homodimeric enzyme distributed widely in nature (Cooper, 1985, and references therein). It catalyzes, via a ping-pong bi-bi kinetic mechanism, the reversible transfer of the γ-amino group of GABA to α-ketoglutarate to yield succinic semialdehyde and L-glutamate, i.e.,

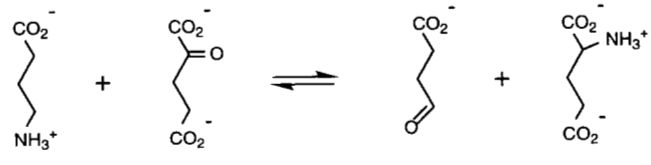

In mammals, GABA-AT plays an important role in the regulation of GABA concentration in the brain (Baxter & Roberts, 1961; Kuriyama et al., 1966), where this molecule is a major inhibitory neurotransmitter (Kuffler & Edwards, 1958). The enzyme is the target of a successful anti-epileptic drug, 4-aminohex-5-enoate, which is also known as vinyl-GABA or Vigabatrin (Mumford & Cannon, 1994).

The structure of GABA-AT is currently under X-ray crystallographic investigation (Marcovic-Housley et al., 1990) but

Reprint requests to: Michael D. Toney, Department of Biochemistry, Albert Einstein College of Medicine, 1300 Morris Park Avenue, Bronx, New York 10461-1602; e-mail: toney@aecom.yu.edu.

Abbreviations: GABA, γ-aminobutyrate; GABA-AT, γ-aminobutyrate aminotransferase (EC 2.6.1.19); DGD, dialkylglycine decarboxylase (EC 4.1.1.64); AAT, aspartate aminotransferase (EC 2.6.1.1); PLP, pyridoxal 5′-phosphate. Residues contributed by the symmetry-related subunit of the dimer are indicated by an asterisk (*) throughout.

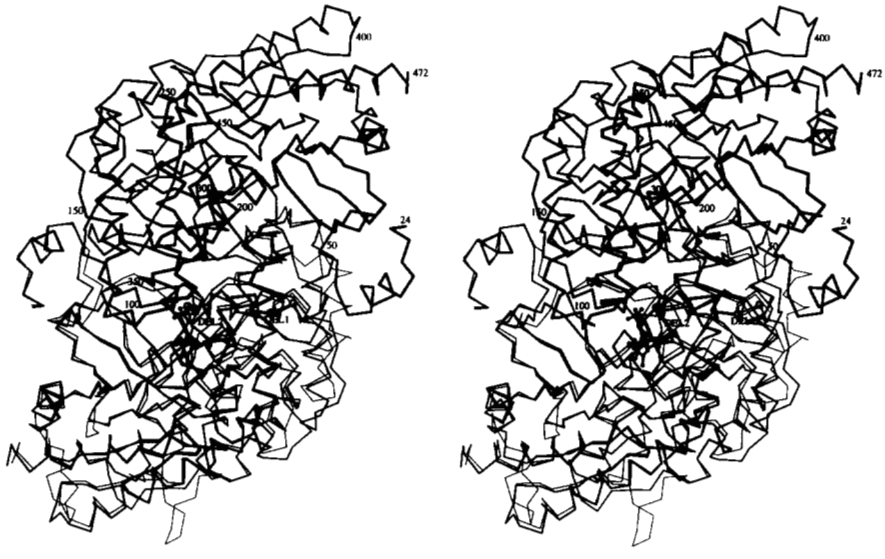

Fig. 1. α-Carbon trace for the GABA-AT dimer homology model. The PLP cofactor and the location of two loops that were replaced by glycines (marked "DEL1" and "DEL2") are shown for one subunit. The DGD monomer (thin lines) is superimposed on the second GABA-AT subunit (thick lines). Every 50th GABA-AT α-carbon is numbered in the first subunit.

is not yet available. GABA-AT belongs to aminotransferase subgroup II, one of four currently recognized subgroups of aminotransferases (Mehta et al., 1993). At least 10 enzymes with approximately 30 known sequences belong to this subgroup. The coordinates for the structure of one of these enzymes, dialkylglycine decarboxylase, are available (Toney et al., 1993, 1995). This abundance of sequence information and the conservation throughout these sequences (Mehta et al., 1993) of several residues found to be in the active site of DGD suggest that homology modeling of the GABA-AT structure could lead to a realistic model for its active site structure.

The homology modeling-deduced active site structure is presented and analyzed in this report. The active site model can explain the stereospecificity of the reactions with natural substrates and also with several inhibitors. Systematic variations in the identities of proposed active site residues within aminotransferase subgroup II correlate well with the apparent functions of these residues deduced from the GABA-AT model and the known substrate specificities of the enzymes. Additionally, once the crystal structure is solved, a comparison of the crystallographic and homology models will provide an indication of the level of reliability of current homology modeling techniques (Bajorath et al., 1993).

Results

The α-carbon tracing for the GABA-AT dimer is shown in Figure 1 and Kinemage 1. It is very similar to those of DGD (Toney et al., 1993, 1995) and ornithine aminotransferase (B. Shen & J.N. Jansonius, pers. comm.), upon which it is based. The locations of the deleted loop regions are marked.

The numbering adopted refers to the mature pig GABA-AT; the corresponding residue numbers for DGD are given in Table 1. Figure 2A presents the active site structure of the GABA-AT model and Kinemage 2; it is compared to that of DGD in Figure 2B. Many of the active site residues that interact directly with PLP and are proposed to be important to the catalytic mechanism of DGD are structurally conserved in the GABA-AT active site: Lys 329 forms a Schiff base linkage with the carbonyl group of PLP, the side-chain amide of Gln 301 donates a hydrogen bond to the 3′ hydroxyl, Asp 298 interacts with the pyridine nitrogen via a hydrogen bond–salt bridge, and Thr 353* donates a hydrogen bond to the phosphate group. Several other residues are also conserved: His 190 and Asn 140 donate hydrogen bonds to Asp 298, Arg 445 can interact with the substrate α-carboxylate, Ser 269 donates a hydrogen bond to the amide oxygen of Gln 301, and Glu 265 and Pro 266 at the bottom of the coenzyme binding pocket perform an indeterminate function.

Two differences in the active site structures of DGD and GABA-AT are deemed to be of primary importance. It has been proposed (Toney et al., 1995) that Gln 52 in DGD donates a hydrogen bond to the substrate α-carboxylate in the decarboxylation half-reaction with dialkylglycines, thereby orienting the external aldimine intermediate properly for scission of the Cα-CO_2^- bond. GABA-AT does not catalyze decarboxylation reactions, which correlates with the observed exchange of Ile 72 for DGD Gln 52. DGD is incapable of using α-ketoglutarate as

Table 1. *Correspondence between the γ-aminobutyrate aminotransferase and dialkylglycine decarboxylase residues discussed in the text*

Conserved		Nonconserved	
GABA-AT	DGD	GABA-AT	DGD
Asn 140	Asn 115	Ile 72	Gln 52
His 190	His 139	Phe 189	Trp 138
Ser 202	Ser 151	Arg 192	Met 141
Glu 265	Glu 210	Lys 203	Ala 152
Ser 269	Ser 214	Glu 270	Ser 215
Asp 298	Asp 243	Val 300	Ala 245
Gln 301	Gln 246	Phe 351	Tyr 301
Lys 329	Lys 272		
Thr 353*	Thr 303*		
Arg 445	Arg 406		

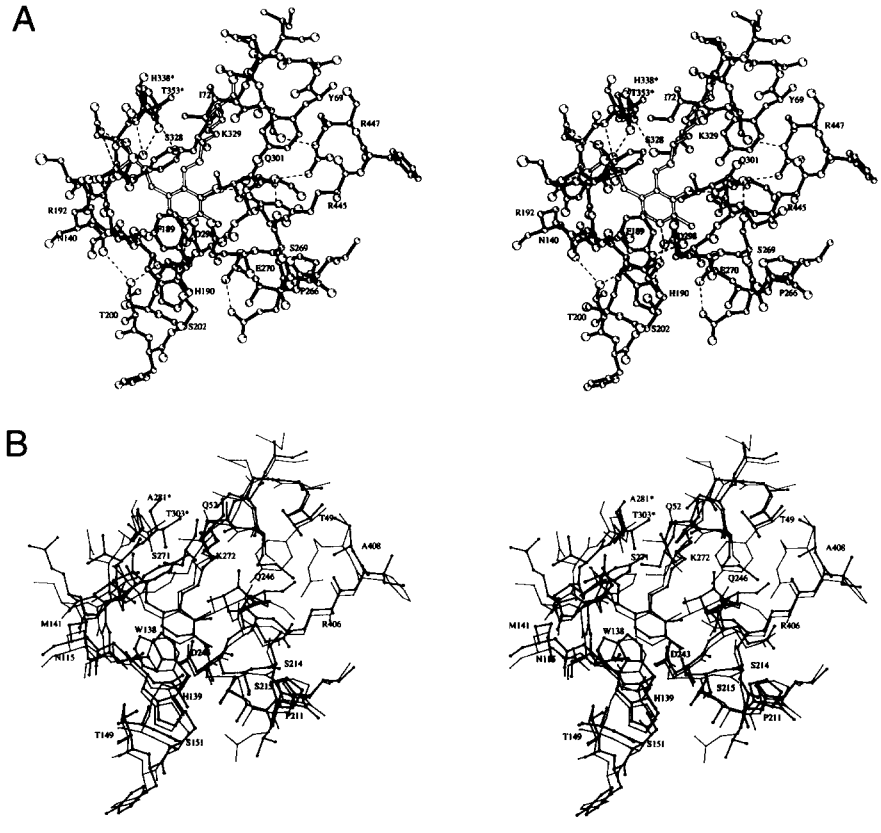

Fig. 2. A: Active site structure for the GABA-AT holoenzyme model. Lys 329 and PLP, which are covalently bonded to one another through a Schiff base linkage, are drawn with open bonds. Potential hydrogen bonds are drawn as dashed lines. **B:** Superimposition of the active site structures of DGD (thick bonds) and the GABA-AT model (thin bonds). Labels are for the DGD structure.

an amino group acceptor in the transamination half-reaction, whereas this α-keto acid is a physiological substrate for GABA-AT. The exchange of Arg 192 for DGD Met 141 probably substantially accounts for this difference. Other amino acid exchanges that are likely to be of secondary mechanistic importance include: Glu 270 in place of DGD Ser 215, Val 300 in place of Ala 245, Phe 189 and Phe 351* in place of Trp 138 and Tyr 301*, respectively, and Lys 203 in place of Ala 152.

The existence of external aldimine intermediates in GABA-AT is dictated by the general mechanism of PLP catalysis (Metzler et al., 1954). Hypothetical external aldimine models for GABA and glutamate are shown in Figure 3 and Kinemage 3. The benzene ring of Phe 189 is rotated forward to accommodate the coenzyme reorientation, which is necessary in order to avoid steric clashes with Lys 329. In the GABA external aldimine model (Fig. 3A), the γ-amino group of the substrate forms a Schiff base with PLP, whereas the carboxylate makes hydrogen bond-salt bridges to Arg 192 and Lys 203. The pro-*S* hydrogen on C4 is oriented perpendicular to the pyridine ring plane. A double hydrogen bond-salt bridge between Arg 445 and Glu 270 is also hypothesized; this would provide charge neutralization, as does the α-carboxylate interaction in the glutamate external aldimine. Jansonius et al. (1994) proposed an analogous interaction for the ornithine aminotransferase catalyzed reaction.

In the glutamate external aldimine model (Fig. 3B), the α-amino group forms a Schiff base with the aldehyde function of PLP, Arg 445 makes a hydrogen bond-salt bridge to the substrate α-carboxylate, and the γ-carboxylate group interacts with Arg 192 and Lys 203 as in the GABA complex. These interactions orient the Cα hydrogen bond perpendicular to the PLP ring plane. Glu 270 is oriented away from Arg 445, so that its carboxylate group accepts a hydrogen bond from Ser 202. It is noteworthy that a model in which Arg 294 replaces Lys 203 in its interaction with the substrate carboxylate group can be built with good geometry and no steric clashes, such that Lys 203 interacts with Glu 270 in the glutamate half-reaction. We feel this model is less likely to reflect the true structures, given the variation in the identity of residue 203 with substrate specificity that is evident in the alignment given in Figure 5.

Hypothetical models for the external aldimines formed with the *S* and *R* isomers of 4-aminohex-5-enoate (vinyl-GABA) are presented in Figure 5 and Kinemage 2. These models are very similar to that for GABA, except for the presence of the vinyl group. This group is oriented toward Arg 445 in the model for the *S* isomer, whereas it is oriented toward Lys 329 in the model for the *R* isomer.

Discussion

It is presently impossible to build a completely accurate model for a chemical structure as complex as GABA-AT without experimental (e.g., X-ray or NMR) data to define it. Given this caveat, we feel that the unavoidable inaccuracies in the side-chain and main-chain positions of a carefully built homology model do not detract from the goal of this study, which is to provide an active site model with correct sequence assignments and generally correct spatial assignments for the main chain and side chains of residues important to the catalytic mechanism and substrate specificity of the enzyme. The value of such a model lies in its explanatory and predictive power. Our confidence that we

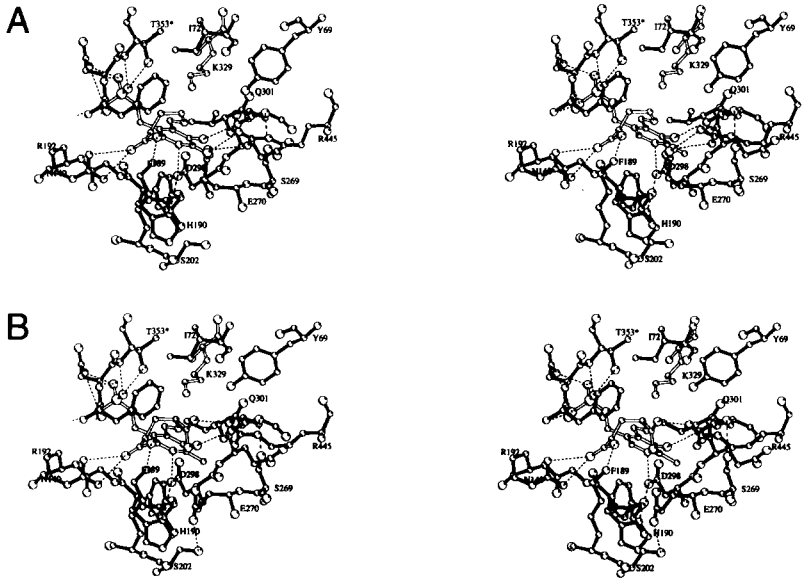

Fig. 3. A: External aldimine model for GABA. The substrate amino group has reacted with the internal aldimine (Lys 329–PLP Schiff base), forming a new bond between GABA and PLP and freeing the ϵ-amino group of Lys 329. The pro-*S* proton of GABA is oriented perpendicular to the plane of the PLP ring and is readily accessible by Lys 329, which is proposed to be the general base catalyst of the 1,3-azaallylic rearrangement interconverting the external aldimine and ketimine intermediates. In this model, specificity for GABA is provided by the ion pair and hydrogen bonding interactions of the GABA carboxylate with Arg 192 and Lys 203. The interaction between Arg 445 and Glu 270 is proposed to be specific to the GABA half-reaction. **B:** External aldimine model for L-glutamate. The model is very similar to that for GABA, except that the substrate α-carboxylate would interact with Arg 445 and Glu 270 would interact with Ser 202.

have achieved this goal is based on sequence alignment information (see below), on the structural integrity of the model, and on the ease with which several pieces of experimental data can be explained by the proposed structure.

Several residues determined experimentally to be at the active site of DGD are completely or highly conserved in aminotransferase subgroup II (Kinemage 2). These include: Gly 111, His 139, Gly 140, Glu 210, Pro 211, Asp 243, Glu 244, Gln 246, Lys 272, Thr 303*, and Arg 406. Three of these (Asp 243, Lys 272, and Arg 406) are invariant among all aminotransferases capable of acting on α-amino acids (Mehta et al., 1993). In the GABA-AT model, these residues are located in positions spatially identical to those in the DGD structure (Fig. 2). Additionally, several nonactive site residues are highly conserved throughout the 28 sequences (representing nine different enzymes) employed in the sequence alignment. These residues, like those in the active site, are not localized but are widely dispersed throughout the sequences. Their correct placement in the GABA-AT structure (with respect to that of DGD) supports the general accuracy of our model. All deletions and insertions in the GABA-AT model, in reference to the DGD structure, occur in loop regions or at the ends of secondary structural elements.

The proposed high degree of tertiary structural conservation between the DGD and GABA-AT active sites, and the observed primary structural conservation of many of these active site residues throughout aminotransferase subgroup II, suggests that the framework provided by the folding pattern of this subgroup requires specific placement of key residues in order to enable transamination. The most critical of these residues are likely to be Lys 329, Asp 298, His 190, and Gln 301. Lys 329, by anal-

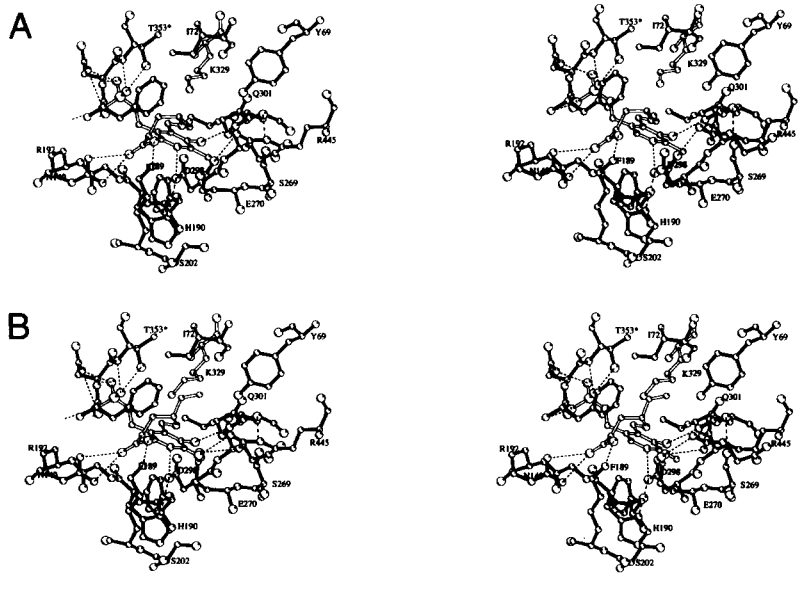

Fig. 4. A: External aldimine model for the *S* isomer of the mechanism-based inhibitor vinyl-GABA. The vinyl group is oriented in the direction of Arg 445. 1,3-Proton transfer from C4 of the inhibitor to C4′ of the coenzyme, which is necessary to activate the molecule as a covalent inhibitor, could readily be accomplished by Lys 329. The presence of the vinyl group would preclude a double hydrogen bond-salt bridge interaction between Glu 270 and Arg 445. **B:** External aldimine model for the *R* isomer of vinyl-GABA. The vinyl group is oriented toward Lys 329. The C4-H bond is oriented toward Arg 445 and is inaccessible by Lys 329, explaining why this isomer is not a covalent inhibitor of GABA-AT.

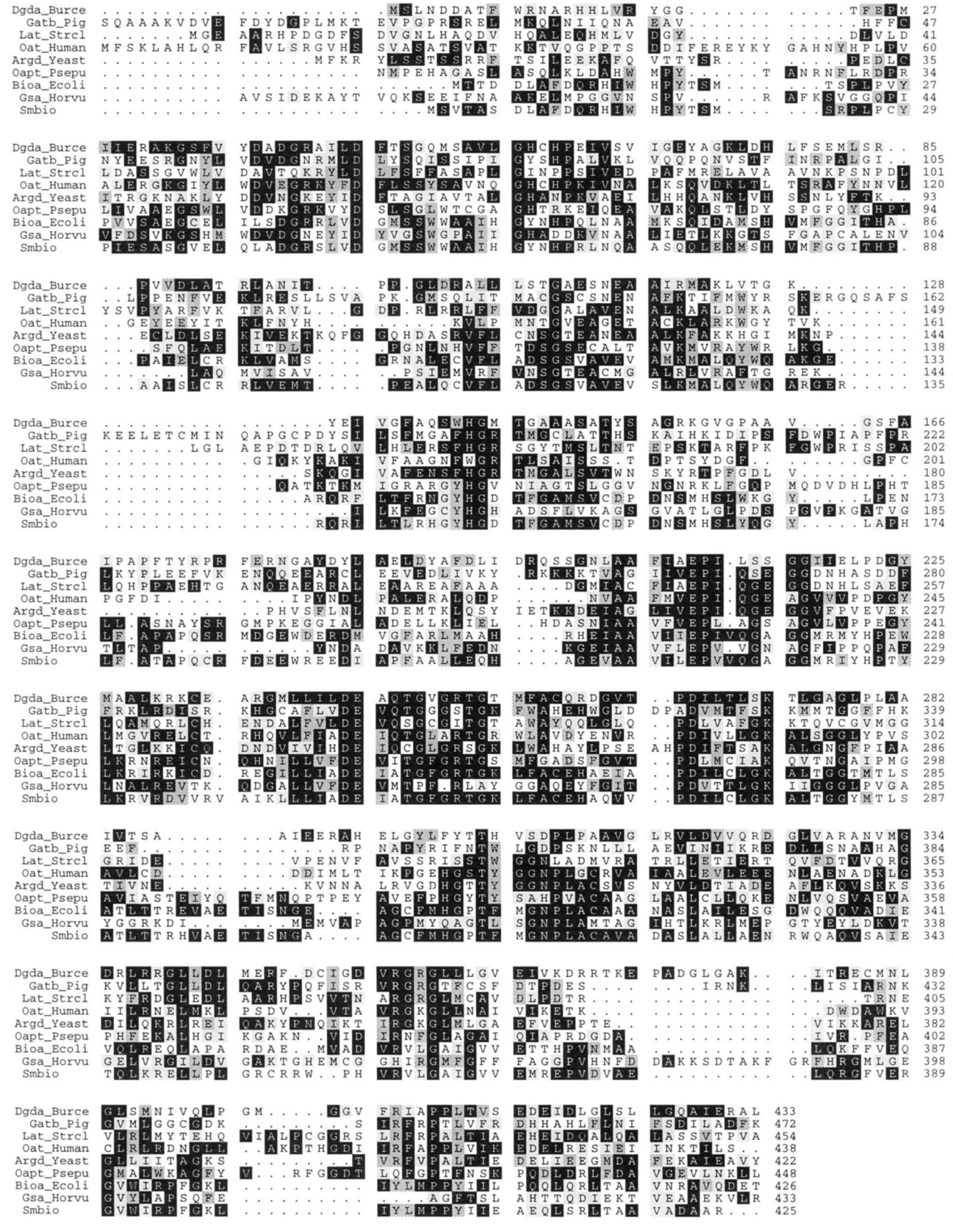

Fig. 5. Aminotransferase subgroup II sequence alignment used in the construction of the GABA-AT homology model and in the analysis of the roles of specific active site residues. One representative sequence for each of the nine distinct enzymes whose sequences are available is shown. Numbering is reported for each sequence in the alignment. The enzymes are labeled with their database codes (see Table 2).

ogy to the function of its structural equivalent (Lys 258) in AAT (Jansonius & Vincent, 1987; Toney & Kirsch, 1993), is probably the general base catalyst for the 1,3-azaallylic rearrangements catalyzed by subgroup II aminotransferases. Additionally, Lys 329 facilitates external aldimine formation by forming a Schiff base with PLP, enabling transamination to occur rather than the inherently slower reaction of the aldehyde with an amino group (Cordes & Jencks, 1962). Again by analogy to structural homologues in AAT, Asp 298, with fine-tuning by His 190 (Yano et al., 1991), would perform the critical function of stabilizing the protonated pyridine nitrogen (Yano et al., 1992) that acts as an electron sink, whereas Gln 301 would lower the pK_a of the internal aldimine to physiologically relevant values (Goldberg et al., 1991).

The GABA external aldimine model (Fig. 3A) explains the observed stereospecificity of GABA-AT and shows several features that are important to the properties of ω-amino acid aminotransferases. GABA-AT is specific for the pro-*S* proton on C4 of GABA. It is this proton in the external aldimine model that is oriented perpendicular to the plane of the pyridine ring, and thus most activated toward removal (Dunathan, 1966). The approximately 30° forward rotation (in the view of Fig. 3) of the coenzyme is immediately apparent, and is similar to that observed experimentally with aspartate aminotransferase (Jansonius & Vincent, 1987; McPhalen et al., 1992; Jäger et al., 1994) and proposed for DGD (Toney et al., 1995). This change in coenzyme orientation is brought about by the formation of an aldimine bond to GABA (displacing Lys 329), by the relief of steric interactions between PLP C4′ and Lys 329 Nϵ once this new bond is formed, and by the relaxation of contacts between the Val 300 side chain and the pyridine ring. This latter interaction may be of general significance to subgroup II aminotransferases. In all subgroup II sequences known to date, except for that of DGD, the position corresponding to Val 300 is either a valine or an isoleucine, whereas in DGD and generally in subgroup I aminotransferases (Mehta et al., 1993) it is an alanine. DGD and subgroup I enzymes act on the proximal groups of α-amino acids, whereas other subgroup II enzymes utilize substrates that lack carboxylate groups located α to the labile amino group. Compared to α-amino acids, amines provide less potential binding energy due to the absence of the α-carboxylate. The strong correlation between β-substitution at position 300 and activity toward ω-amino acids suggests that the strained steric interaction between Val 300 and the pyridine ring, as compared to the unstrained DGD Ala 245 interaction, promotes external aldimine formation by destabilizing the internal aldimine. This may be necessary in order both to speed the rate of formation of the external aldimine intermediate and to lower the dissociation constant for GABA to physiologically relevant levels. That external aldimine formation in GABA-AT is rapid compared to proton abstraction is suggested by the similar deuterium kinetic isotope effects on k_{cat} and k_{cat}/K_m for GABA and the large magnitude of these effects (~7; Yu et al., 1987).

The interaction between Glu 270 and Arg 445 is likely to be important to ω-amino acid half-reactions of subgroup II aminotransferases; Glu 270 is strictly conserved in enzymes that act on ω-amino acids in the first half-reaction and α-amino acids in the second, whereas it is a neutral amino acid in others (e.g., DGD, glutamate semialdehyde aminotransferase). The proposed charge-neutralizing hydrogen bond–salt bridge between these residues in the GABA external aldimine would largely take the place of the Arg 445–α-carboxylate interaction in the glutamate external aldimine (see below). It is tempting to speculate on a detrimental influence of an uncompensated Arg 445 positive charge on the pK_a of Lys 329 in the external aldimine, on the external aldimine conformation, or on the stability of a reactive intermediate.

Lys 203 could interact directly with the bound substrates via the carboxylate distal to the reactive amino group. This suggestion is strengthened by the fact that in ornithine and lysine ϵ-aminotransferases, which act on the ω-amino groups of α-amino acids, either glutamate or aspartate is uniformly exchanged for Lys 203, implying a role for this residue in binding the unreactive α-amino group in these enzymes.

The active site region of the GABA-AT model is quite "open" compared to the closed form of AAT (McPhalen et al., 1992). Although the present model does not provide evidence for a substrate-dependent conformational change in GABA-AT and one is yet to be observed with DGD, several experimental approaches have provided such evidence (D.S. Kim & Churchich, 1982, 1987; Y.T. Kim & Churchich, 1991; Choi & Churchich, 1985a, 1985b). For example, experiments on the inactivation of GABA-AT by bis-PLP (D.S. Kim & Churchich, 1982; Y.T. Kim & Churchich, 1991) show differential protection by GABA and α-ketoglutarate. The latter completely prevents inactivation, suggesting a conformational change given that, in the present model, the lysine residue modified by this reagent is distant from the active site.

It is suggested that the hydrogen bond–salt bridge formed between the glutamate α-carboxylate and Arg 445 leads to a reorientation of Glu 270 such that it hydrogen bonds to Ser 202. The conformational switch from the Glu 270–Arg 445 interaction in the ω-amino acid half-reaction (see above) to the Glu 270–Ser 202 interaction in the α-amino acid half-reaction may be a key factor in the ability of certain subgroup II aminotransferases to utilize both types of substrates via a single active site. Residues capable of donating a hydrogen bond to Glu 270 are conserved (serine, threonine, asparagine, or glutamine) at the position corresponding to Ser 202 in the other aminotransferases (i.e., ornithine, *N*-acetylornithine, and lysine ϵ-aminotransferase) that act on ω-amino groups in the first half-reaction and α-amino groups in the second.

Silverman et al. (1987) reported on the reactivities of several β-substituted phenyl and *p*-chlorophenyl analogues of GABA. Their results show that although both the *R* and *S* isomers bind to the enzyme with similar affinities, only the *S* isomers undergo turnover (20–70-fold slower than GABA). The GABA external aldimine model (Fig. 3A) provides a basis for understanding these results. The *S* isomers would bind with the phenyl group oriented snugly between Ile 72 and Phe 351*, sterically unencumbered after minor rearrangement in these side chains. The *R* isomers, on the other hand, would bind with the phenyl group oriented toward the PLP phosphate group; the steric interactions incurred in this region would necessitate a severe reorientation in the position of the GABA backbone, leading to an aldimine conformation unfavorable for external aldimine deprotonation. The similar affinity of the enzyme for the *R* and *S* isomers would be fortuitous given their different binding modes. No detailed model for the high-affinity binding mode of the *R* isomer is proffered, but one possibility is that interaction of the phenyl group with Phe 189 and the carboxylate group with Arg 445 would occur.

Vinyl-GABA, known clinically as Vigabatrin, is a drug widely used for the control of epileptic seizures (Mumford & Cannon, 1994). It covalently inactivates GABA-AT, and the mechanism of this reaction has been elucidated (De Biase et al., 1991). The *S* isomer is active, whereas the *R* is inactive toward GABA-AT. Vigabatrin is a mechanism-based inhibitor. It forms an external aldimine intermediate that, like the natural substrates, undergoes a general base-catalyzed 1,3-azaallylic rearrangement to a ketimine intermediate. Unlike the natural substrates, Vigabatrin yields an α,β-unsaturated ketimine that reacts via Michael addition with Lys 329, producing an enamine that then tautomerizes. The proposed structures for the Vigabatrin external aldimine intermediates (Fig. 4) provide an explanation for the isomeric specificity. Only in the model for the *S* isomer is the C4-H bond oriented perpendicular to the pyridine ring plane, readily accessible by the Lys 329 ϵ-amino group that is proposed to be the general base catalyst in the reaction of the natural substrates (see above). In the external aldimine model for the *R* isomer, on the other hand, the C4-H bond is not accessible to Lys 329 (Fig. 4B). Rather, it is oriented toward Glu 270, whereas the vinyl group would be perpendicular to the pyridine ring plane and directed toward Lys 329, which would change conformation to accommodate the substituent. This configuration would preclude the Lys 329 catalyzed 1,3-azaallylic rearrangement necessary to the activation of the molecule as an inhibitor.

In summary, the homology model presented for the GABA-AT active site can explain the substrate specificity and stereospecificity of the enzyme, as well as its reactivity toward several substituted GABA analogues. In conjunction with the sequence alignment and substrate specificities of the aligned enzymes, the model identifies residues that (1) are involved in determining the ability of certain subgroup II aminotransferases to utilize primary amines in one half-reaction and α-amino acids in another, and (2) provide specificity for the substrate functional groups that are distal to the reactive center. The model can additionally account for the unique reactivity of the *S* compared to the *R* isomer of Vigabatrin as a mechanism-based inhibitor. It is hoped that, in the absence of an experimentally determined structure for GABA-AT, this model will prove useful to the future design of GABA-AT inhibitors and provide a foundation upon which site-directed mutagenesis studies aimed at delineating the roles of active site residues can be based.

Methods

All of the protein sequences used herein (except that of human GABA-AT; De Biase et al., 1995) were obtained from the Swiss-Prot (release 28), EMBL DataLib (release 38), or GenBank (release 82) databases, and are for proteins that belong to the aminotransferase subgroup II (Mehta et al., 1993). These sequences were aligned using PILEUP (default settings) of the GCG sequence analysis software package (Genetics Computer Group, 1991). The sequences aligned for the determination of residues conserved in aminotransferase subgroup II are listed in Table 2. A portion of this full sequence alignment (one representative sequence for each enzyme included) is given in Figure 5. The three-dimensional structure of DGD (Toney et al., 1993, 1995) served as the template upon which the GABA-AT model was built. Profile analysis demonstrated that DGD is a representative member of aminotransferase subgroup II, and that its closest relative in subgroup II is GABA-AT from *Escherichia coli* (Mehta & Christen, 1994). Additionally, the α-carbon tracing of human ornithine aminotransferase was provided by B. Shen and J.N. Jansonius of the Biozentrum der Universität Basel, Switzerland.

The HOMOLOGY module of the program INSIGHTII (Biosym, 1993) was used for model construction and initial refinement. The final stages of refinement employed the programs O (Jones & Kjelgaard, 1990) and XPLOR (Brünger, 1990).

Structurally conserved regions of the DGD structure were determined by overlaying the α-carbon traces of DGD and ornithine aminotransferase using the structure-based alignment procedure in HOMOLOGY. This algorithm overlays structures based on residues (up to 40) in an active box that is superimposed on the sequence alignment. These regions were conservatively assigned because only two α-carbon traces were available for this family of enzymes. The coordinates for the DGD atoms in the sequence regions designated as structurally conserved were then transferred to the corresponding GABA-AT atoms. Atoms in GABA-AT residues that had no correspondents in the aligned DGD residues were assigned so that the side chains were in extended conformations.

Loop regions were obtained by searching the Brookhaven Protein Data Bank for structural fragments that bridged the residues adjacent to the loops (whose coordinates had already been assigned) with an acceptable geometry. The loop regions chosen from this survey of the data bank were generally those with the lowest RMS difference in backbone coordinates for the overlapping regions and the highest sequence homology.

Two loops in GABA-AT that are much smaller in DGD were judged too large to model accurately. We decided to replace these loop sequences with two glycine residues, given that our interest lies mainly in the active site structure and that these loops are distant from the active site. The glycines provide flexible connections between the flanking residues and introduce neither restrictions on the structures of these regions nor strain. The loop regions that were deleted are: Arg 152–Asp 179 and Phe 213–Phe 220. No attempt was made to model the N-terminal region up to Pro 23.

Initially, the structure of the GABA-AT monomer was constructed and refined by automated rotamer optimization followed by energy minimization. Automated rotamer optimizations were performed for approximately 100 residues simultaneously; it was not possible to include the complete molecule due to computer hardware limitations. GABA-AT is known to be dimeric. The transformation matrix that relates the two monomers in the twofold symmetric DGD dimer (DGD is tetrameric, a dimer of dimers; Toney et al., 1993, 1995) was calculated, and this was applied to the GABA-AT coordinates in order to generate the initial GABA-AT dimer. At this point, there were several unacceptable steric clashes at the dimer interface. The dimer was manually rebuilt using the program O, optimizing all hydrogen bonds and ionic interactions and relieving steric clashes by manipulating side-chain conformations. This was followed by 200 cycles of twofold symmetry-restrained energy minimization in XPLOR. Manual rebuilding and energy minimization were repeated three more times.

The final model has no steric clashes as determined by XPLOR. It meets the criteria proposed by Morris et al. (1992) for an accurate protein model, which has narrow distributions of both amino acid side-chain torsion angles and hydrogen bond

Table 2. *Subgroup II sequences included in the multiple sequence alignment*

Swiss-Prot or GenEmbl code	Enzyme	Source	EC number
Argd_Ecoli	Acetylornithine aminotransferase	*Escherichia coli*	EC 2.6.1.11
Argd_Yeast	Acetylornithine aminotransferase	*Saccharomyces cerevisiae*	EC 2.6.1.11
Bioa_Bacsh	Adenosylmethionine-8-amino-7-oxononanoate aminotransferase	*Bacillus sphaericus*	EC 2.6.1.62
Bioa_Ecoli	Adenosylmethionine-8-amino-7-oxononanoate aminotransferase	*Escherichia coli*	EC 2.6.1.62
Dgda_Burce	Dialkylglycine decarboxylase	*Pseudomonas cepacia*	EC 4.1.1.64
Gabt_Ecoli	4-Aminobutyrate aminotransferase	*Escherichia coli*	EC 2.6.1.19
Gata_Emeni	4-Aminobutyrate aminotransferase	*Aspergillus nidulans*	EC 2.6.1.19
Gata_Yeast	4-Aminobutyrate aminotransferase	*Saccharomyces cerevisiae*	EC 2.6.1.19
Gatb_Pig	4-Aminobutyrate aminotransferase	*Sus scrofa*	EC 2.6.1.19
Gatb_Human	4-Aminobutyrate aminotransferase	*Homo sapiens*	EC 2.6.1.19
Gsa_Bacsu	Glutamate-1-semialdehyde 2,1-aminomutase	*Bacillus subtilis*	EC 5.4.3.8
Gsa_Ecoli	Glutamate-1-semialdehyde 2,1-aminomutase	*Escherichia coli*	EC 5.4.3.8
Gsa_Horvu	Glutamate-1-semialdehyde 2,1-aminomutase	*Hordeum vulgare*	EC 5.4.3.8
Gsa_Salty	Glutamate-1-semialdehyde 2,1-aminomutase	*Salmonella typhimurium*	EC 5.4.3.8
Gsa_Synp6	Glutamate-1-semialdehyde 2,1-aminomutase	*Synechococcus*	EC 5.4.3.8
Gsa_Tobac	Glutamate-1-semialdehyde 2,1-aminomutase	*Nicotiana tabacum*	EC 5.4.3.8
XPHEML	Glutamate-1-semialdehyde 2,1-aminomutase	*Xanthomonas phaseoli*	EC 5.4.3.8
CRO3632	Glutamate-1-semialdehyde 2,1-aminomutase	*Chlamydomonas reinhardtii*	EC 5.4.3.8
GMGSA	Glutamate-1-semialdehyde 2,1-aminomutase	*Glycine max*	EC 5.4.3.8
Lat_Nocla	Lysine-ε-aminotransferase	*Nocardia lactamdurans*	EC 2.6.1.36
Lat_Strcl	Lysine-ε-aminotransferase	*Streptomyces clavuligerus*	EC 2.6.1.36
Oapt_Psepu	ω-Amino acid:pyruvate aminotransferase	*Pseudomonas putida*	EC 2.6.1.18
Oat_Human	Ornithine aminotransferase	*Homo sapiens*	EC 2.6.1.13
Oat_Mouse	Ornithine aminotransferase	*Mus musculus*	EC 2.6.1.13
Oat_Rat	Ornithine aminotransferase	*Rattus norvegicus*	EC 2.6.1.13
Oat_Vigac	Ornithine aminotransferase	*Vigna aconitifolia*	EC 2.6.1.13
Oat_Yeast	Ornithine aminotransferase	*Saccharomyces cerevisiae*	EC 2.6.1.13
SMBIO	7,8-Diamino-pelargonic acid aminotransferase	*Serratia marcescens*	EC 2.6.1.62

energies. The 3D-1D profiles (Bowie et al., 1991) for the GABA-AT and DGD models are very similar in form.

Models for the obligatory external aldimine intermediates were built based on the structure of the holoenzyme, and on coenzyme rearrangements that have been observed experimentally in aspartate aminotransferase structures (Jansonius & Vincent, 1987; McPhalen et al., 1992; Jäger et al., 1994). The complete holoenzyme model and the active site regions of the external aldimine models are available upon request to the authors. Stereo pictures presented in this report were made with MOLSCRIPT (Kraulis, 1991).

Acknowledgments

Professors D. Barra and F. Bossa of the Università di Roma provided critical guidance and support for this work, which has been partially supported by grants from the Italian MURST and CNR (Progetto Speciale Bioinformatica). We are grateful to Professor J.N. Jansonius for access to the computer facilities in his laboratory, in the framework of an EEC Human Capital and Mobility project (contract ERBCHRXCT930179), and to Dr. B. Shen for providing α-carbon coordinates for human ornithine aminotransferase. We thank Professors R.A. John and J.N. Jansonius for helpful suggestions and critical reading of the manuscript.

References

Bajorath J, Stenkamp R, Aruffo A. 1993. Knowledge-based model building of proteins: Concepts and examples. *Protein Sci 2*:1798–1810.

Baxter MG, Roberts E. 1961. Elevation of gamma-aminobutyric acid in brain: Selective inhibition of gamma-aminobutyric-alpha-ketoglutaric transaminase. *J Biol Chem 236*:3287–3294.

Biosym. 1993. *Manual for InsightII.* San Diego, California: Biosym Technologies, Inc.

Bowie JU, Lüthy R, Eisenberg D. 1991. A method to identify protein sequences that fold into a known three-dimensional structure. *Science 235*:164–170.

Brünger AT. 1990. *X-PLOR manual.* New Haven, Connecticut: Yale University Press.

Choi SY, Churchich JE. 1985a. 4-Aminobutyrate aminotransferase reaction of sulfhydryl residues connected with catalytic activity. *J Biol Chem 260*:993–997.

Choi SY, Churchich JE. 1985b. 4-Aminobutyrate aminotransferase. Conformational changes induced by reduction of pyridoxal 5-phosphate. *Biochim Biophys Acta 830*:120–126.

Cooper AJ. 1985. Glutamate-gamma-aminobutyrate transaminase. *Methods Enzymol 113*:80–82.

Cordes EH, Jencks WP. 1962. Semicarbazone formation from pyridoxal, pyridoxal phosphate, and their Schiff bases. *Biochemistry 1*:773–780.

De Biase D, Barra D, Bossa F, Pucci P, John RA. 1991. Chemistry of the inactivation of 4-aminobutyrate aminotransferase by the antiepileptic drug Vigabatrin. *J Biol Chem 266*:20056–20061.

De Biase D, Barra D, Simmaco M, John RA, Bossa F. 1995. Primary structure and tissue distribution of human 4-aminobutyrate aminotransferase. *Eur J Biochem 227*:476–480.

Dunathan HC. 1966. Conformation and reaction specificity in pyridoxal phosphate enzymes. *Proc Natl Acad Sci 55*:712–716.

Genetics Computer Group. 1991. *Program manual for the GCG package version 7.3.* Madison, Wisconsin: Genetics Computer Group.

Goldberg JM, Swanson RV, Goodman HS, Kirsch JF. 1991. The tyrosine-225 to phenylalanine mutation of *Escherichia coli* aspartate aminotransferase results in an alkaline transition in the spectrophotometric and kinetic pK_a values and reduced values of both k_{cat} and K_m. *Biochemistry 30*:305–312.

Jäger J, Moser M, Sauder U, Jansonius JN. 1994. Crystal structures of *Escherichia coli* aspartate aminotransferase in two conformations. Compar-

ison of an unliganded open and two liganded closed forms. *J Mol Biol 239*:285–305.

Jansonius JN, Genovesio-Taverne JC, Hennig M, Hohenester E, Jenny M, Malashkevich VN, Moser M, Muller R, Shen BW, Stark W, von Stosch A, Toney MD. 1994. Crystallographic studies on the vitamin B_6-assisted enzyme transamination reaction. In: Marino G, Sannia G, Bossa F, eds. *Biochemistry of vitamin B6 and PQQ*. Basel: Birkhauser-Verlag. pp 29–35.

Jansonius JN, Vincent MG. 1987. Structural basis for catalysis by aspartate aminotransferase. In: Jurnak FA, McPherson A, eds. *Biological macromolecules & assemblies, vol 3*. New York: Wiley & Sons. pp 187–288.

Jones TA, Kjelgaard M. 1990. *Manual for O*. Uppsala: Uppsala University.

Kim DS, Churchich JE. 1982. 4-Aminobutyrate aminotransferase, reaction of P'P2-bis(5'-pyridoxal) diphosphate with lysyl residues connected with catalytic activity. *J Biol Chem 257*:10991–10995.

Kim DS, Churchich JE. 1987. The reversible oxidation of vicinal SH groups in 4-aminobutyrate aminotransferase. Probes of conformational changes. *J Biol Chem 262*:14250–14254.

Kim YT, Churchich JE. 1991. 4-Aminobutyrate aminotransferase: Identification of lysine residues connected with catalytic activity. *Biochim Biophys Acta 1077*:187–191.

Kraulis J. 1991. MOLSCRIPT: A program to produce both detailed and schematic plots of protein structures. *J Appl Crystallogr 24*:946–950.

Kuffler SW, Edwards C. 1958. Mechanism of gamma aminobutyric acid (GABA) action and its relation to synaptic inhibition. *J Neurophysiol 21*:589–610.

Kuriyama K, Roberts E, Rubinstein MK. 1966. Elevation of gamma-aminobutyric acid in brain with amino-oxyacetic acid and susceptibility to convulsive seizures in mice: A quantitative re-evaluation. *Biochem Pharmacol 15*:221–236.

Marcovic-Housley Z, Schirmer T, Fol B, Jansonius JN, De Biase D, John RA. 1990. Crystallization and preliminary X-ray analysis of gamma-aminobutyric acid transaminase. *J Mol Biol 214*:821–823.

McPhalen CA, Vincent MG, Picot D, Jansonius JN, Lesk AM, Chothia C. 1992. Domain closure in mitochondrial aspartate aminotransferase. *J Mol Biol 227*:197–213.

Mehta PK, Christen P. 1994. Homology of 1-aminocyclopropane-1-carboxylate synthase, 8-amino-7-oxononanoate synthase, 2-amino-6-caprolactam racemase, 2,2-dialkylglycine decarboxylase, glutamate-1-semialdehyde 2,1-aminomutase and isopenicillin-*N*-epimerase with aminotransferases. *Biochem Biophys Res Commum 198*:138–143.

Mehta PK, Hale TI, Christen P. 1993. Aminotransferases: Demonstration of homology and division into evolutionary subgroups. *Eur J Biochem 214*:549–561.

Metzler DE, Ikawa M, Snell EE. 1954. A general mechanism for vitamin B_6-catalyzed reactions. *J Am Chem Soc 76*:648–656.

Morris AL, MacArthur MW, Hutchinson EG, Thorton GM. 1992. Stereochemical quality of protein structure coordinates. *Proteins Struct Funct Genet 12*:345–364.

Mumford JP, Cannon DJ. 1994. Vigabatrin. *Epilepsia 35*(Suppl 5):25–28.

Silverman RB, Invergo BJ, Levy MA, Andrew CR. 1987. Substrate stereospecificity and active site topography of gamma-aminobutyric acid aminotransferase for beta-aryl-gamma-aminobutyric acid analogues. *J Biol Chem 262*:3192–3195.

Toney MD, Hohenester E, Cowan SW, Jansonius JN. 1993. Dialkylglycine decarboxylase structure: Bifunctional active site and alkali metal sites. *Science 261*:756–759.

Toney MD, Hohenester E, Keller JW, Jansonius JN. 1995. Structural and mechanistic analysis of two refined crystal structures of the pyridoxal phosphate-dependent enzyme dialkylglycine decarboxylase. *J Mol Biol 245*:151–179.

Toney MD, Kirsch JF. 1993. Lysine 258 in apartate aminotransferase: Enforcer of the Circe effect for amino acid substrates and general base catalyst for the 1,3-prototropic shift. *Biochemistry 32*:1471–1479.

Yano T, Kuramitsu S, Tanase S, Morino Y, Hiromi K, Kagamiyama H. 1991. The role of His 143 in the catalytic mechanism of *Escherichia coli* aspartate aminotransferase. *J Biol Chem 266*:6079–6085.

Yano T, Kuramitsu S, Tanase S, Morino Y, Kagamiyama H. 1992. Role of Asp 222 in the catalytic mechanism of *Escherichia coli* aspartate aminotransferase: The amino acid residue which enhances the function of the enzyme-bound coenzyme pyridoxal 5'-phosphate. *Biochemistry 31*: 5878–5886.

Yu PH, Durden DA, Davis BA, Boulton AA. 1987. Deuterium isotope effect in gamma-aminobutyric acid transamination: Determination of rate-limiting step. *J Neurochem 48*:440–446.